

# Plaquette valence-bond ordering in $J_1 - J_2$ Heisenberg antiferromagnet on the honeycomb lattice

H. Mosadeq\*,<sup>1</sup> F. Shahbazi†,<sup>1</sup> and S.A. Jafari‡<sup>1,2,3</sup>

<sup>1</sup>Department of Physics, Isfahan University of Technology, Isfahan 84156-83111, Iran

<sup>2</sup>Department of Physics, Sharif University of Technology, Tehran 11155-9161, Iran

<sup>3</sup>School of Physics, Institute for Research in Fundamental Sciences (IPM), Tehran 19395-5531, Iran

(Dated: April 2, 2024)

We study  $S = 1/2$  Heisenberg model on the honeycomb lattice with first and second neighbor antiferromagnetic exchange ( $J_1 - J_2$  model), employing exact diagonalization in both  $S_z = 0$  basis and nearest neighbor singlet valence bond (NNVB) basis. We find that for  $0.2 < J_2/J_1 < 0.3$ , NNVB basis gives a proper description of the ground state in comparison with the exact results. By analysing the dimer-dimer as well as plaquette-plaquette correlations and also defining appropriate structure factors, we investigate possible symmetry breaking states as the candidates for the ground state in the frustrated region. We provide body of evidences in favor of plaquette valence bond ordering for  $0.2 < J_2/J_1 < 0.3$ . By further increasing the ratio  $J_2/J_1$ , this state undergoes a transition to the staggered dimerized state.

PACS numbers: 75.10.Jm 75.10.Kt, 75.40.Mg

## I. INTRODUCTION

Quantum spin liquid (QSL) is non magnetic state of a correlated matter for which there is no broken symmetry in the spin part of the ground state wave function. Hence the local magnetic moments remain disordered down to absolute zero ( $T = 0$ )[1]. The quantum ground state for QSL can be expressed as the superposition of many different configurations, such as linear combinations of the short range singlet valence bonds. This state is called resonating valence bond (RVB), originally proposed by Fazekas and Anderson as the ground state of the Heisenberg model on the triangular lattice [2]. The singlet bonds in RVB state can be considered as pre-formed Cooper pairs, which under suitable conditions (*i.e.* hole doping) may coherently propagate throughout the system, hence give rise to superconductivity [3].

Many strongly correlated systems are well described by Hubbard Hamiltonian whose ground state for large on site coulomb interaction is the Mott insulating state. In this state the electrons are localized on the atoms, nevertheless local charge fluctuations induce an Anti-ferromagnetic (AF) exchange interaction between the spins of the electrons. Hence, AF Heisenberg model is an effective Hamiltonian for describing the low energy excitations of the Mott insulators [4]. It has been proved that in 1D, the Ground state of the Heisenberg model is a gapless (critical) spin liquid for  $S = 1/2$ -chain, while it is gapped spin liquid for  $S = 1$ -chain [5]. Finding the realizations of QSL in two and three dimensions has been the subject of many researches in recent years [1]. Quantum fluctuations as well as frustration may destroy the long range magnetic order in spin systems. When a spin system is frustrated, it can not find a spin configuration to fully satisfy the interaction between each pair of spins. There are two mechanisms for frustration: (i) Geometrical frustration, where the

lattice geometry is such that, it is not possible to minimize the interaction energy of all bonds at the same time, *e.g.* in triangular or Kagomé lattice in 2D and pyrochlore lattice in 3D [6]. (ii) When there are several competing exchange interactions, such as competition between first and second neighboring AF exchange interactions ( $J_1 - J_2$  model). Since the quantum fluctuations are larger in 2D, many attempts to find QSL are focused on the quasi two-dimensional frustrated spin systems with  $S = 1/2$  [7].

Two dimensional Heisenberg antiferromagnets apart from their own importance [4], received intensive attention in the context of layered high- $T_c$  superconducting (HTSC) material [3]. The ground state of  $S = 1/2$  Heisenberg model with AF nearest neighbor (NN) exchange coupling on 2D bipartite lattices has been shown to be Néel ordered [8–14]. Addition of next nearest neighbor (NNN) AF interactions frustrates the system and gradually destroys the (Néel) order. Since AF exchange interaction encourages the singlet formation, the quantum ground state of AF Heisenberg model can be expressed in term of over complete set of valence bond (VB) basis which represent a total spin singlet state [15].

The  $J_1 - J_2$  AF Heisenberg model on square lattice has been extensively studied and various VB states have been proposed to describe its disorder regime [16]. One example of such quantum states is nearest neighbor RVB (NNRVB) representing a spin liquid, which breaks neither translational nor rotational symmetries. However, in highly frustrated regime where the ground state is classically disordered and the SU(2) symmetry of the Hamiltonian is restored, there is no theorem to prevent breaking of the lattice translational symmetry. Therefore, in spite of earlier proposal of states with no symmetry breaking [17], states which break translational symmetry were proposed [18–20]. One example is the staggered dimerized state which breaks translational and rotational symmetries of the lattice. Another candidate, that has been proposed recently for some lattices, is plaquette RVB (PRVB) wave functions in which the resonance of VBs is limited to one plaquette [21–25]. PRVB state breaks the translational symmetry, while preserves the rotational symmetry of the lattice.

\*h-mosadeq@ph.iut.ac.ir

†shahbazi@cc.iut.ac.ir

‡akbar.jafari@gmail.com

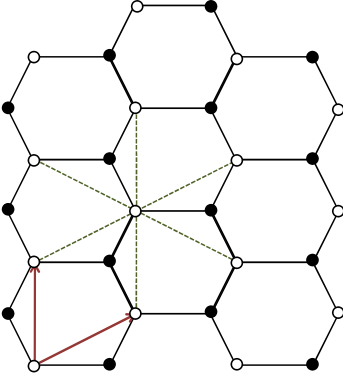


FIG. 1: The bipartite honeycomb lattice. Two sublattices are marked by black and white circles. Nearest neighbor lattice points are connected with solid lines and next to nearest neighbor lattice points are connected with dashed lines. Red arrows show the two primitive lattice vectors.

Recent fabrication of graphene monolayer and also magnetic compounds with quasi 2D honeycomb structure, has brought the honeycomb lattice to attention of the physicists from both experimental and theoretical points of view. Honeycomb lattice does have coordination number equal to three, which is minimum among two-dimensional lattices. In the case of Heisenberg model on honeycomb lattice, the small number of neighboring interactions enhances the quantum fluctuations and therefore seems to be promising system to explore spin liquid states. Honeycomb lattice is a bipartite lattice composed of two interlacing triangular sublattices (Fig. 1). The unit cell of this non-bravais lattice contains two sites and lattice is constructed by two lattice vectors of the triangular bravais lattice. The non-bravais character of lattice results in more exotic aspects that can not be seen in square lattice or the other bravais lattices [26].

As some realizations of Heisenberg magnets on the honeycomb lattice, one can name recently discovered compounds such as  $\text{InCu}_{2/3}\text{V}_{1/3}\text{O}_3$  [28] and  $\text{Na}_3\text{Cu}_2\text{SbO}_6$  [27] in which the  $\text{Cu}^{+2}$  ions in the copper-oxide layers form a two-dimensional  $S = 1/2$  Heisenberg antiferromagnet on a honeycomb lattice,  $\text{Bi}_3\text{Mn}_4\text{O}_{12}(\text{NO}_3)$  (BMNO) in which the  $\text{Mn}^{+4}$  ions with  $S = 3/2$  reside on the lattice points of weakly coupled honeycomb layers [29]. Replacing  $\text{Mn}^{+4}$  with  $\text{V}^{+4}$  in this compound may realize the  $S = 1/2$  Heisenberg model on honeycomb lattice. Also the recent progress in the field of ultracold atoms and trapping techniques [30] along with the ability to tune the interaction parameters via the Feshbach resonance [31] can be thought of another way to realize Heisenberg spins (of localized fermions) on a honeycomb optical lattice.

Two recent achievements has raised the hope of finding QSL in honeycomb geometries. One, is the large scale quantum Monte Carlo simulation of the half-filled Hubbard model on the honeycomb lattice, which results a spin liquid phase with finite spin gap for moderate values of on-site coulomb interaction ( $3.5 < U/t < 4.3$ ). This phase is located be-

tween the semi-metallic phase characterized by massless dirac fermions ( $U/t < 3.4$ ) and the AF-Mott insulating phase for  $U/t > 4.3$  [32]. The other is the experimentally observed spin liquid behavior in BMNO which remains magnetically disordered down to  $T = 0.4\text{K}$ , in spite of its high Curi-Weiss temperature  $T_{\text{CW}} \approx -257\text{K}$  [29].

Motivated by the above considerations, in this paper we investigate the ground state properties of  $J_1 - J_2$  Heisenberg model which is proposed for explaining the spin liquid behavior of BMNO. The paper is organized as follows. In section. II we introduce the spin Hamiltonian and using diagonalization in nearest neighbor VB basis, we find evidence for spin liquid phase for a range of coupling constants. In section. III we employ the exact diagonalization in full Hilbert space of  $S_z = 0$ . With exact wave-functions obtained in this manner, we calculate the dimer-dimer correlation function. We find two different quantum phases in frustrate regime. In section. IV by introducing suitable structure factors, quantum phase transition point is determined. At the end, in section. V, we calculate plaquette-plaquette correlations which points to a possible PRVB state. Section. VI is devoted to discussion and conclusion.

## II. MODEL HAMILTONIAN AND ITS GROUND STATE CANDIDATES

$J_1 - J_2$  AF Heisenberg Hamiltonian is defined by,

$$\mathcal{H} = J_1 \sum_{\langle i,j \rangle} \mathbf{S}_i \cdot \mathbf{S}_j + J_2 \sum_{\langle\langle i,j \rangle\rangle} \mathbf{S}_i \cdot \mathbf{S}_j, \quad (1)$$

in which  $J_1 > 0$  and  $J_2 > 0$  are AF exchange interactions between first and second neighboring spins, respectively. The first sum is limited to NN sites, while the second sum runs over the NNN lattice sites. Since the square lattice is connected with high  $T_c$  superconducting materials, the studies of frustrated phases of spin models has been usually limited to this lattice. Recently discovered magnetic materials with underlying honeycomb geometry is our motivation to study the above model on the honeycomb lattice.

Using effective action approach to the frustrated Heisenberg antiferromagnet in two dimensional system, Einarsson *et. al.* proved that the  $S = 1/2$  disorder ground state on the honeycomb lattice is three-fold degenerate [33]. Fouet *et. al.* [34] provided some evidence for staggered dimerized (SD) state for  $S = 1/2$  at  $J_2/J_1 = 0.4$ . Such state breaks the rotational lattice symmetry ( $C_3$ ), while preserves its translational symmetry (Fig. 2). They also speculated that spin liquid phase and PRVB phases can be stabilized for some range of  $J_2/J_1$  (Fig 3). PRVB phase breaks the translational symmetry, but preserves the rotational symmetry of lattice. Alternatively, Read and Sachdev [35] used large  $N$  expansion method, proposed another ground state wave function which breaks both the translational and the rotational symmetries of the lattice (Fig 4).

In the classical limit (large spins), it has been shown that the ground state of the above model is Néel ordered for

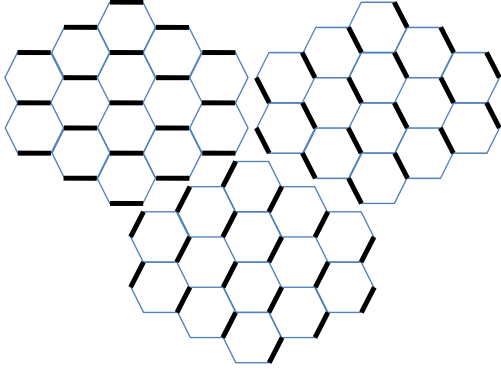


FIG. 2: Three degeneracy of staggered dimerized wave function on honeycomb lattice.

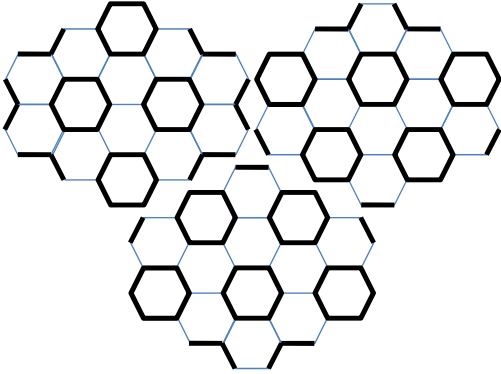


FIG. 3: Three degeneracy of Plaquette Valence Bond wave function on honeycomb lattice.

$J_2/J_1 < 1/6$  while for  $J_2/J_1 > 1/6$  the ground state consists of an infinitely degenerate set of spiral states characterized by spiral wave vectors  $\mathbf{q}$  [36]. Okumura et al [37] used a combination of low temperature expansion and Monte Carlo simulation showed that thermal fluctuations can lift the huge degeneracy of the ground state, leading to a state with broken  $C_3$  symmetry of honeycomb lattice. According to their finding, in the vicinity of Néel phase boundary, the energy scale associated with the thermal order-by-disorder becomes so small that exotic spin liquid behavior, such as ring-liquid or pancake-liquid can emerge. Mulder *et. al.* argued that taking the quantum fluctuations into account, some specific wave vectors in this manifold are picked as the ground state – a manifestation of order by disorder mechanism. They find for  $S = 1/2$  quantum fluctuations are strong enough to destroy the spiral order and stabilize the valence bond solid with staggered ordering [38]. Our aim in this paper is to study the ground state of model (1) using exact diagonalization in both  $S_z$  and nearest neighbor valence bond (NNVB) basis.

### III. DIAGONALIZATION IN NNVB BASIS

The valence bond states are a subset of  $S_z=0$  basis with total spin magnitude  $S^2$  equal to zero. In this section we show

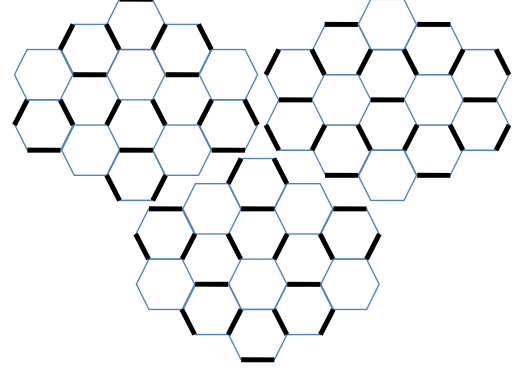


FIG. 4: Three degeneracy of wave function proposed by Read and Sachdev on honeycomb lattice.

that the ground state of the  $J_1 - J_2$  Heisenberg model in the frustrated regime, where there is no long range order, can be very well approximated in terms of states in NNVB subspace.

Let us expand the ground state wave function in terms of NNVB states as

$$|\psi_0\rangle = \sum_{\alpha} a(c_{\alpha}) |c_{\alpha}\rangle, \quad (2)$$

where  $|c_{\alpha}\rangle$  denotes all possible configurations  $\alpha$  of NNVBs:

$$|c_{\alpha}\rangle = \prod_{(i,j) \in \alpha} (i_{\uparrow} j_{\downarrow} - i_{\downarrow} j_{\uparrow}). \quad (3)$$

First, we have to enumerate the basis  $|c_{\alpha}\rangle$  to construct a numerical representation of the Hamiltonian matrix in this basis. To determine the basis, the exact Pfaffian representation of the RVB wave function is employed [39]. In this method one expresses the RVB wave function as the Pfaffian of an antisymmetric matrix whose dimension is equal to the number of lattice points. The NNVB basis is much smaller than the whole  $S_z = 0$  basis, so that the Hamiltonian matrix can be fully diagonalized with standard library routines. Note that since the NNVB states ( $|c_{\alpha}\rangle$ ) are not orthonormal, one needs to solve the generalized eigen-value problem

$$\det[\mathcal{H} - E\mathcal{O}] = 0,$$

where  $\mathcal{O} = \langle c_{\beta} | c_{\alpha} \rangle$  denotes the overlap matrix of the NNVB configurations.

In the upper panel of Fig. 5 we have compared ground state energies obtained in the NNVB basis, and those obtained by numerically exact diagonalization in the  $S_z = 0$  basis versus  $J_2/J_1$ . In the middle panel we show the relative error in the ground state energy and the lower panel shows the overlap of the exact ground state wavefunction with the ground state obtained within NNVB basis set. As can be seen in this figure, the agreement between the two sets of energies for  $J_2/J_1 \in ]0.2, 0.3[$  is remarkable. Since the NNVB basis is not complete, the large error obtained by NNVB basis for  $J_2/J_1 < 0.2$  and  $J_2/J_1 > 0.3$  can be attributed to the fact that longer range valence bonds start to contribute. For  $J_2/J_1 < 0.2$ , where there is Néel order in the ground

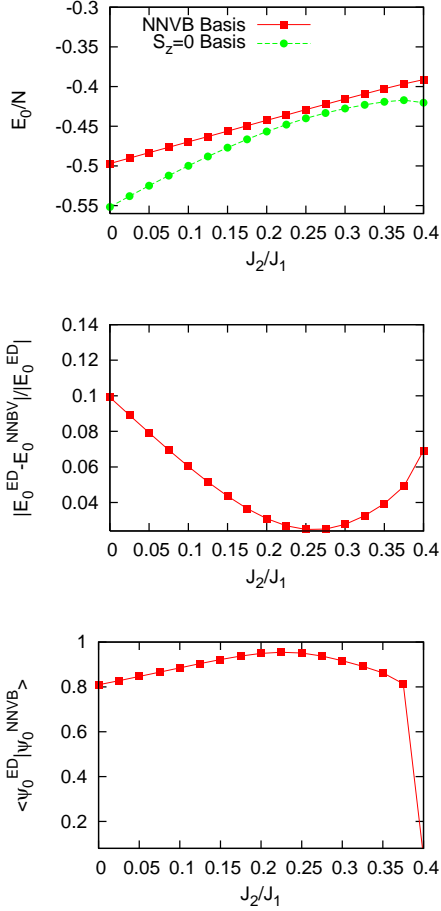


FIG. 5: Up: The comparison between the exact ground state energy evaluated using exact diagonalization in  $S_z=0$  basis (squares) and diagonalization in NNVB basis (circles) as a function of  $J_2/J_1$ . middle: The relative errors between the ground state energies obtained by the two basis sets defined as  $(E_0^{\text{NNVB}} - E_0^{\text{ED}})/(E_0^{\text{ED}})$ . Down: The overlap of the exact GS wavefunction  $|\psi_0^{\text{ED}}\rangle$  with the GS wavefunction obtained in NNVB basis  $|\psi_0^{\text{NNVB}}\rangle$ .

state, it was shown that long-ranged VB states have remarkable contribution in the ground state wave function [40]. Starting from  $J_2/J_1 = 0$ , the Néel order is destroyed by increasing frustration strength up to  $J_2/J_1 \approx 0.2$ . At this point, the spin-spin correlations will become short ranged and the nature of the ground state can be accurately captured by NNVB wave functions. For  $J_2/J_1 > 0.3$ , the frustrating second neighbor AF exchange coupling  $J_2$  induces singlet formation between next nearest neighbors (NNNB's) which compete with NNVB's. Therefore in this region the NNVB basis is insufficient to capture the true ground state. Furthermore, upon increasing  $J_2/J_1$  beyond 0.35, as will be shown shortly, the nearest neighbor singlets in the VB states (dimers) will start to become correlated.

The RVB wave function (QSL) is defined as linear superposition of all possible VB configurations with the same am-

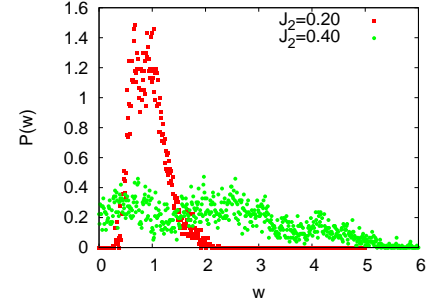


FIG. 6: Probability distribution of the relative amplitudes of VB's in the ground state wave-function for  $J_2/J_1 = 0.2, 0.4$  and cluster size  $N = 54$ .

plitude. Thus it can be represented as:

$$|RVB\rangle = A \sum_{\alpha} |c_{\alpha}\rangle, \quad (4)$$

in which  $A = \frac{1}{(\sum_{\alpha, \alpha'} \langle c_{\alpha} | c_{\alpha'} \rangle)^{1/2}}$  is the normalization coefficient. In order to get preliminary insight into the nature of the ground state obtained in NNVB basis, we compare the distribution of the amplitudes of VB configurations in eq. (2) to the uniform amplitude  $A$  of the above RVB liquid state. For this purpose we define the ratio  $w(c_{\alpha}) = \frac{a(c_{\alpha})}{A}$ , and look at the distribution of relative weights,  $w$ . If the ground state has the characteristics of a RVB spin liquid, this distribution is expected to be sharply peaked around  $w = 1$ . In Fig. 6 we plot the probability distribution function (PDF) of the relative amplitudes  $w$  for  $J_2/J_1 = 0.2$  and  $J_2/J_1 = 0.4$  in a cluster of  $N = 54$  spins. As can be seen in this figure, for  $J_2/J_1 = 0.2$  the PDF is narrower relative to  $J_2/J_1 = 0.4$ , which implies that the ground state for  $J_2/J_1 = 0.2$  is more similar to spin liquid state. The broader distribution of amplitudes for  $J_2/J_1 > 0.4$  on the other hand, indicates significant deviation from QSL behavior, which can be considered as a sign of symmetry breaking. To investigate the effect of finite lattice geometry on the ground state, we compare PDFs of rel-

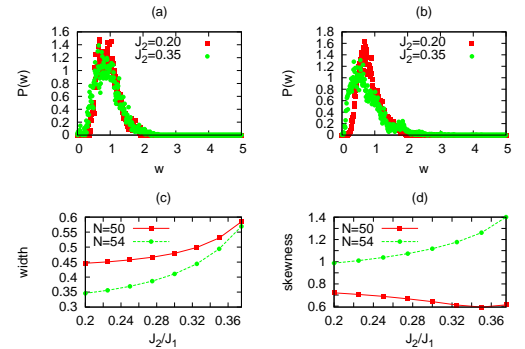


FIG. 7: (Color online) PDF of relative amplitude  $w$  for  $J_2/J_1 = 0.2, 0.35$  for (a)  $N = 50$  and (b)  $N = 54$ . (c) Width and (d) skewness of PDF vs.  $J_2/J_1$  for  $N = 50, 54$ .

Trial state	$\psi_{\text{SD}}$			$\psi_{\text{PL}}$						$\psi_{\text{RS}}$					
$\langle P_\alpha \rangle_{\text{avg}}$	0			-0.106(5)						0					
$\alpha'$	$\beta$	$\gamma$	$\delta$	$\beta$		$\gamma$		$\delta$		$\beta$		$\gamma$		$\delta$	
$\langle P_\alpha P_{\alpha'} \rangle_1$	+1/4	+1/4	+1/4	-	-	-	-	-	-	-1/2	1	-1/2	+1/4	-1/2	1
$\langle P_\alpha P_{\alpha'} \rangle_2$	+1/4	+1/4	-1/2	-	-	-	-	-	-	+1/4	+1/4	-1/2	1	-1/2	+1/4
$\langle P_\alpha P_{\alpha'} \rangle_3$	+1	+1	-1/2	-	-	-	-	-	-	-1/2	+1/4	+1/4	+1/4	+1/4	+1/4
$\langle P_\alpha P_{\alpha'} \rangle_{\text{avg}}$	<b>1/2</b>	<b>1/2</b>	<b>-1/4</b>	-	-	-	-	-	-	<b>-1/4</b>	<b>+1/2</b>	<b>-1/4</b>	<b>+1/2</b>	<b>-1/4</b>	<b>+1/2</b>
$C(\alpha, \alpha')$	1/2	1/2	-1/4	-0.090(5)	0.170(8)	-0.090(5)	0.170(8)	-0.090(5)	0.170(8)	-1/4	+1/2	-1/4	+1/2	-1/4	+1/2

TABLE I:  $\langle P_\alpha P_{\alpha'} \rangle - \langle P_\alpha \rangle \langle P_{\alpha'} \rangle$  for  $\alpha$  fixed and  $\alpha' = \beta, \gamma, \delta$  (Fig. 8). Three indices 1, 2, 3 refer to three degenerate states (cf. Figs. 2, 3, 4) which become orthogonal to each other in the thermodynamic limit for pure SD and RS states. Subscript *avg* denotes average over these three possible degeneracies. Since the three degenerate PL states are not orthogonal to each other in the thermodynamic limit, in this case the correlations have been extracted from finite size scaling of the numeric data. Digits in the parenthesis denote errors in the last digit.

ative amplitudes for two cluster sizes  $N = 50$  and  $N = 54$ , and  $J_2/J_1 = 0.2$  and  $J_2/J_1 = 0.35$ . These are shown in the two top panels of Fig. 7. It can be easily seen that for the lattice size  $N = 50$ , the PDFs are more symmetric than  $N = 54$ . This can be attributed to the fact that, in contrast to the cluster with  $N = 50$  lattice points, the plaquette wave function can be fitted to the cluster with  $N = 54$  subject to the periodic boundary condition. Therefore the symmetry breaking toward plaquette formation is more pronounced for  $N = 54$ . This signals a tendency for plaquette formation, provided it is compatible with the lattice geometry. Moreover for  $N = 54$ , increasing the value of  $J_2$  leads to emergence of a second peak at the right tail of PDF. The average of relative amplitudes of VB configurations taking part in the plaquette wave function turns out to be 1.56. Interestingly, position of the second peak is quite close to this values. Therefore, the second peak can be attributed to the amplification of plaquette character in the ground state, as a result of increasing the second neighbor exchange interaction. To quantify the variations of PDF ( $p(w)$ ) versus  $J_2/J_1$ , we compute its width given by the standard deviation ( $\sigma = \langle (w - \langle w \rangle)^2 \rangle^{1/2}$ ) and also its skewness defined by  $\frac{\langle (w - \langle w \rangle)^3 \rangle}{\sigma^3}$ . Panel (c) of Fig. 7 is plot of width versus  $J_2/J_1$  for  $N = 54$ , showing that the width of PDF increases monotonically from  $J_2/J_1 = 0.2$  to  $J_2/J_1 = 0.4$ . The panel (d) in this figure, represents the rise of PDF skewness for  $N = 54$  in terms of  $J_2/J_1$ , indicating that by increasing  $J_2$  the distribution functions for this size get more and more asymmetric, while for  $N = 50$  skewness does not change remarkably. This suggests that the skewness can be considered as a heuristic indication of possible symmetry breaking. In summary, since the widths of PDFs considered here are finite for the interval  $0.2 \lesssim J_2/J_1 \lesssim 0.35$ , the above arguments suggest that the ground state of  $J_1 - J_2$  model in this interval is not a perfect QSL state. A more precise understanding of the ground state properties, requires the study the correlation between dimers. This will be done in the following section.

#### IV. EXACT DIMER-DIMER CORRELATIONS

In this section, employing exact diagonalization we obtain the ground state in  $S_z = 0$  basis. Using the exact wave function of the ground state, we calculate correlation between

dimers for  $0.2 \lesssim J_2/J_1 \lesssim 0.5$ . The dimer-dimer correlation is defined by,

$$C(\alpha, \alpha') = 4(\langle (\mathbf{S}_i \cdot \mathbf{S}_j)(\mathbf{S}_k \cdot \mathbf{S}_l) \rangle - \langle (\mathbf{S}_i \cdot \mathbf{S}_j) \rangle \langle (\mathbf{S}_k \cdot \mathbf{S}_l) \rangle), \quad (5)$$

where  $\alpha' = (k, l)$ , and  $\alpha = (i, j)$  is the reference bond relative to which the correlations are calculated. Define the permutation operator by,

$$P_{kl} = 2(\mathbf{S}_k \cdot \mathbf{S}_l) + \frac{1}{2}, \quad (6)$$

in terms of which Eq. (5) can be alternatively expressed as

$$C(\alpha, \alpha') = \langle P_\alpha P_{\alpha'} \rangle - \langle P_\alpha \rangle \langle P_{\alpha'} \rangle. \quad (7)$$

In table I quantities  $C(\alpha, \alpha')$  for fixed  $\alpha$  and  $\alpha' = \beta, \gamma, \delta$  (Fig. 8) are shown for three trial wave functions  $\psi_{\text{SD}}$ ,  $\psi_{\text{PL}}$  and  $\psi_{\text{RS}}$ , where RS, SD and PL stands for Read-Sachdev, staggered dimerized, and plaquette states, respectively. The expectation values of the operator  $\langle P_{\alpha'} \rangle$  for each of the three degenerate SD and RS states is  $-1$  if bond  $\alpha'$  is occupied by a dimer, and  $+1/2$ , otherwise.  $\langle P_{\alpha'} \rangle_{\text{avg}}$  in table I is obtained by averaging over three degenerate states corresponding to SD and RS trial wavefunction. For PL trial state, since the three degenerate configurations are not orthogonal in thermodynamic limit, the averaging is not valid and we compute  $C(\alpha, \alpha')$  numerically by finite size scaling method. Fig. 9 gives a graphical representation of the correlations obtained in this way. Red and blue links denote positive and negative correlations, and their thickness is proportional to the magnitude of correlations with the reference bond  $\alpha$  of Fig. 8. The reference bond  $\alpha$  is denoted by a double line in Fig. 9. It can be

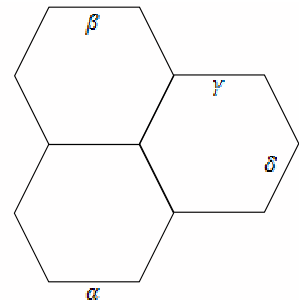


FIG. 8: The reference bond  $\alpha$ , and three independent bonds  $\beta, \gamma, \delta$ .



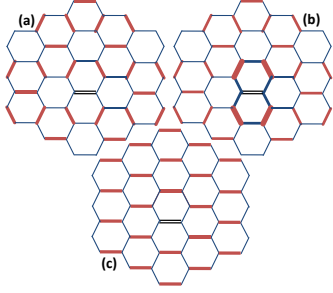


FIG. 9: Snapshots of correlations corresponding from left to right to (a) RS, (b) PL, and (c) SD trial states. Red and blue links correspond to positive and negative correlations with respect to reference bond  $\alpha$  which has been denoted by double line.

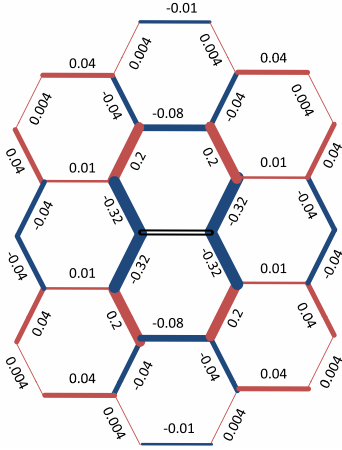


FIG. 10: The dimer-dimer correlation for honeycomb lattice with periodic boundary condition at  $J_2 = 0.3$ . Red (Blue) lines denote positive (negative) correlation. The thickness of lines is proportional to the magnitude of correlations. The system size is  $N = 32$ .

seen in this figure that the pattern for the sign of correlations in PL and RS states are identical, except for their magnitudes. Specifically, in the PL state, the magnitudes of correlations between the dimers which belong to the same hexagon as the reference bond, are stronger than the rest of dimers. But in the RS state all dimers have identical correlation with respect to the reference bond.

In Fig. 10 and Fig. 11, we have shown the exact diagonalization results for the *dimer-dimer* correlation functions at  $J_2/J_1 = 0.3$  and  $J_2/J_1 = 0.4$ , respectively for a lattice with  $N = 32$  sites, subject to periodic boundary conditions. Note that in order to implement symmetries of infinite lattice on finite size systems, the size  $N$  is limited to specific numbers  $N = 24, 32, 42, 50, 54, \dots$ . Since the dimension of Hilbert space grows exponentially with  $N$ , the exact diagonalization in the whole  $S_z = 0$  subspace is not feasible, and hence for  $N > 32$  we carried out the calculations in NNVB basis. The correlations are computed with respect to the middle-bond indicated by double lines. Red bonds denote positive correla-

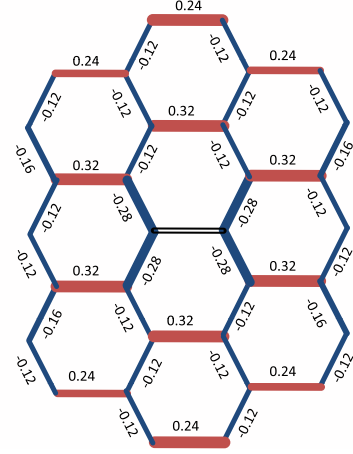


FIG. 11: The dimer-dimer correlation for honeycomb lattice with periodic boundary condition at  $J_2 = 0.4$ . Red (Blue) lines denote positive (negative) correlation. The thickness of lines is proportional to the magnitude of correlations. The system size is  $N = 32$ .

tions, while the blue ones indicate negative correlations. The thickness of bonds are proportional to the magnitude of correlations. As can be seen in Fig. 10, for  $J_2/J_1 = 0.3$ , the correlations are decaying with distance (measured with respect to central bond). Comparing this correlation map with Fig. 9(b), shows remarkable similarity to the snapshot corresponding to PL ordering.

The dimer-dimer correlation pattern at  $J_2/J_1 = 0.4$  shown in Fig. 11 is entirely different. First the dimer-dimer correlations do not appreciably decay over the maximum distance displayed in the figure. Second, one can easily distinguish a staggered ordering pattern by noting that, correlations between bonds parallel to the reference dimer are positive, while others are negatively correlated with the reference dimer. Comparing with Fig. 9 (c), this correlation snapshot obviously suggests a staggered dimerized state at  $J_2/J_1 = 0.4$ . This is in agreement with previous study of Fouet and coworkers [34]. However, Fouet *et al.* speculated that at  $J_2/J_1 = 0.3$  the correlation pattern resembles a RS state. Based on qualitative symmetry consideration of short-range dimer-dimer correlations, Fouet and coworkers proposed the possibility of crystal of hexagon plaquettes as a candidate for the ground state in the  $0.3 < J_2/J_1 < 0.35$  range [34]. In the following we demonstrate that for  $0.2 \lesssim J_2/J_1 \lesssim 0.3$ , the dominant correlations are of PL type, rather than RS.

For quantitative characterization of the nature of VB crystalline state, we define the following structure factor:

$$S_\lambda = \sum_{\alpha'} \varepsilon_\lambda(\alpha') C(\alpha, \alpha'), \quad (8)$$

where  $C(\alpha, \alpha')$  is given by Eq. (7) and  $\varepsilon_\lambda(\alpha')$  is the phase factor, appropriately defined for each of the three states  $\lambda \equiv \text{SD}, \text{PL}, \text{RS}$  [24]. The phase factors  $\varepsilon_{\text{SD}}, \varepsilon_{\text{PL}}$  and  $\varepsilon_{\text{RS}}$  are shown in Fig. 12. Since the sign of dimer-dimer correlations for PL and RS states are the same, their phase factors must be equal. Scaling behavior of  $S_\lambda$  for a lattice with  $N$  sites and  $N_b$  bonds

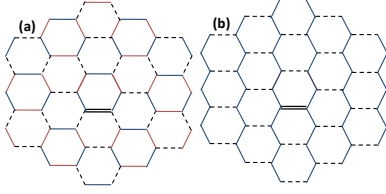


FIG. 12: Red and blue links correspond to  $+1$ ,  $-1$  phase factors, respectively, while the dashed links stand for 0. Reference dimer is identified by double link. (a) Phase factor convention for PL and RS states. (b) Phase factors for staggered dimerized state.

is given by,

$$\frac{S_\lambda}{N_b} = C_\lambda^\infty + \frac{A}{N}. \quad (9)$$

Using the above phase factors, and the correlations  $C(\alpha, \alpha')$  given in table I we have calculated the corresponding  $C_\lambda^\infty$  in table II for each of the three trial states  $\psi_\lambda$ .

In Fig. 13 we have shown  $S_{SD}$  and  $S_{PL}$  versus  $J_2/J_1$  for  $N = 24, 42, 54$ . Note that for  $N = 24$ , we have done exact diagonalization in  $S_z = 0$  basis, while for  $N = 42, 54$ , NNVB basis has been used. Note that the NNVB calculations is valid only in the region  $0.2 < J_2/J_1 < 0.35$ . With these three sizes, we have performed finite size scaling according to Eq. (9) to obtain  $C_{SD}^\infty$  and  $C_{PL}^\infty$ . Fig. 13(a) and (b) show SD and PL structure factors, respectively, for various sizes. For values of  $J_2/J_1 \gtrsim 0.35$  we do not have reliable data for  $N = 42, 54$ . Hence we have not reported finite size scaling for these values of  $J_2/J_1$ . For  $0.2 < J_2/J_1 < 0.35$ , the SD structure factor in (a) remains much smaller than  $C_{SD}^\infty = 1/4$  (table II) for all three sizes. On the other hand, the PL structure factor in (b) can be extrapolated to a finite value between 0.07 and 0.1 (empty squares) which are comparable with the exact value 0.125 of the pure PL state (table II).

A sudden jump observed in Fig. 13 (a) and (b) suggests the existence of a first order phase transition from PL to SD state as one increases  $J_2/J_1$  beyond a certain value between 0.35 and 0.4. In panels (b) of Fig. 13 the average ratio of structure factor (averaged over the range  $0.2 < J_2/J_1 < 0.35$ ) to the corresponding  $C_{PL}^\infty$  is given by  $(S_{PL}/N_b)/C_{PL}^\infty \approx 0.66$ , while this ratio for RS state in the same region is  $(S_{RS}/N_b)/C_{RS}^\infty \approx 0.08/0.375 \approx 0.21$ . Hence for  $0.2 < J_2/J_1 < 0.35$  we expect the ground state to be dominated by plaquette valence bond order.

TABLE II: Intensive structure factor in thermodynamic limit for the three trial states.

Trial state	$\psi_{SD}$	$\psi_{PL}$	$\psi_{RS}$
$C_{SD}^\infty$	1/4	0	0
$C_{PL}^\infty$	0	0.125(5)	3/8

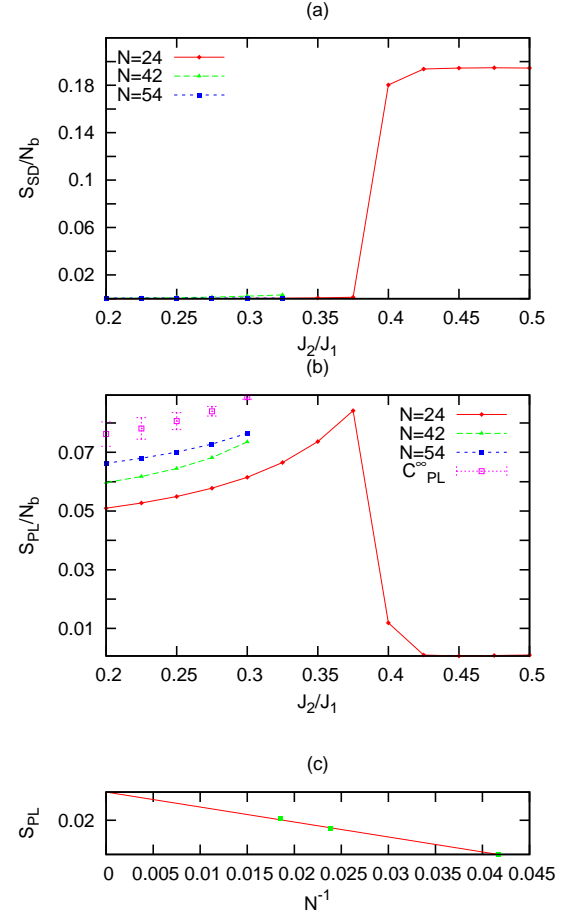


FIG. 13: The structure factor computed for lattice with  $N = 24$  (diamond),  $N = 42$  (triangle) and  $N = 54$  (square).  $N_b$  stand for the number of dimers. Structure factors correspond to (a) Staggered dimerized state, (b) Plaquette state. In (b), empty square with error bar indicates extrapolation to infinite lattice size. (c) shows a finite size scaling according to Eq. (9) for PL structure factors and  $J_2/J_1 = 0.3$ . As can be seen for a specific value of  $J_2/J_1$  between 0.35 and 0.4, there is a sudden increase for SD structure factor, which is accompanied by a sudden decrease in the PL structure factor.

In addition we calculated the exact value of  $\langle P_{\alpha'} \rangle$  as a function of  $J_2/J_1$  for  $N = 24$  sites. For  $J_2/J_1$  from 0.2 to 0.35, the expectation value  $\langle P_{\alpha'} \rangle$  increases monotonically from  $-0.21$  to  $-0.12$  and shows a sudden jumps to 0.001 for  $J_2/J_1 = 0.4$ . In view of the  $\approx -0.1$  value for the expectation value of permutation operator in the PL state (table I), the negative values in the range  $0.2 < J_2/J_1 < 0.35$  can be considered as an extra support in favor of plaquette valence bond solid in this regime. Guided by the above evidences for plaquette ordering in region  $0.2 < J_2/J_1 < 0.35$ , in the next section we calculate the plaquette-plaquette correlation using exact diagonalization method.

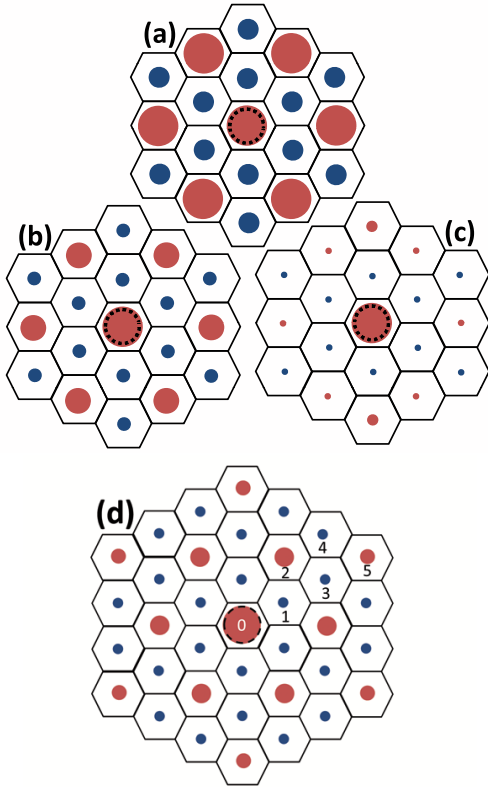


FIG. 14: Red (blue) circles denote positive (negative) correlations. The radius of circles are proportional to the value of plaquette-plaquette correlation. The reference plaquette is depicted by black dashed line. (a) The plaquette-plaquette correlation map calculated for PL trial state. The exact plaquette-plaquette correlation evaluated using exact diagonalization on honeycomb lattice for (b)  $J_2/J_1 = 0.3$  and (c)  $J_2/J_1 = 0.5$ . (d) PL-PL correlation pattern for  $N = 54$  and  $J_2/J_1 = 0.3$ .

## V. PLAQUETTE ORDER IN FRUSTRATED REGIME

A more direct tool to detect plaquette ordering in frustrated regime is to investigate the plaquette-plaquette correlation defined by,

$$C(p, q) = \langle Q_p Q_q \rangle - \langle Q_p \rangle^2, \quad (10)$$

$$Q_p = \frac{1}{2}(\Pi_p + \Pi^{-1}_p),$$

where  $p, q$  stand for different plaquette and  $\Pi$  ( $\Pi^{-1}$ ) is the cyclic exchange operator which permutes six spins around a hexagon in clockwise (counter-clockwise) direction. This correlation function was introduced recently and has been used to investigate plaquette ordering in frustrated Heisenberg magnets on the checkerboard and square lattice [21–23, 25].

In Fig. 14-(a) we have depicted the plaquette correlation in PL state. Red (blue) circles indicate positive (negative) correlations, with the radii of circles are proportional to the magnitude of correlation. The reference plaquette is marked with a dashed circle. Fig. 14-(b) and (c) represent the plaquette correlation function obtained by exact diagonalization

TABLE III: Relative plaquette-plaquette correlations for hexagons with different distance to reference hexagon.

$C(i,0)/C(0,0)$	$\psi_{\text{PL}}$	$\psi_{\text{RVB}}$	$\psi_{\text{ED}}$
$i = 1$	-0.12	-0.04	-0.08
$i = 2$	0.28	0.13	0.175
$i = 3$	-0.12	-0.04	-0.07
$i = 4$	-0.12	-0.008	-0.05
$i = 5$	0.28	0.05	0.11

in  $S_z = 0$  basis for  $N = 24$  sites at  $J_2/J_1 = 0.3, 0.5$ , respectively. Comparison of panels (b) and (c) of Fig. 14 with panel (a), indicates substantial PL ordering at  $J_2/J_1 = 0.3$ . It is remarkable to note that even the ratio of strengths of positive and negative correlations in (b) ( $\sim 0.29 : 0.14$ ) and (a) ( $0.35 : 0.13$ ) agree with each other. This ratio in (c) becomes  $0.04 : 0.04$  which significantly deviates from the corresponding value for a pure PL state (a). Fig. 14(d) is the same as (b), for larger size  $N = 54$  and  $J_2/J_1 = 0.3$ . As can be seen, for  $N = 54$  too, a substantial plaquette correlation pattern can be observed. Moreover, for this size we calculated the PL-PL correlations for all hexagons (denoted by 1,2,3,4,5 in Fig. 14(d)) with respect to the reference one to which, number 0 is assigned. In last column of table III we have listed the relative correlations, defined by  $C(i,0)/C(0,0)$ , obtained by exact diagonalization in NNVB basis and compare them with corresponding values for PL and RVB states given in first and second columns, respectively. As can be seen, for RVB state this quantity decays rapidly with distance from the reference hexagon, while the exact data does not show such a rapid decaying. This again is an evidence in favor of the PL nature of the ground state.

## VI. CONCLUSION

In summary, diagonalization of  $J_1 - J_2$  antiferromagnet Heisenberg Hamiltonian on honeycomb lattice in both  $S_z=0$  basis and NNVB basis show a striking agreement between these two approaches in the parameter range  $0.2 < J_2/J_1 < 0.3$ . Therefore, in this region the ground state can be well described in terms of the singlet bonds between the nearest neighbor spins. Analysis of the exact dimer-dimer correlations, structure factors, and also plaquette-plaquette correlations, suggests the existence of plaquette valence bond crystal in this range of couplings. In fact the emergence of such PL ordering can be attributed to the quantum fluctuations due to the tendency of second neighbors to form singlets. This study also reveals a phase transition from the plaquette ordered to the staggered dimerized state at a point in the interval  $J_2/J_1 \in [0.35, 0.4]$ . Similar results, regarding plaquette ordering on the square lattice, have been previously obtained for  $J_1 - J_2 - J_3$  Heisenberg antiferromagnet in its maximally frustrated region,  $J_2 + J_3 \sim J_1/2$ , and for  $J_2 \leq J_3$  [24]. Our results are in contrast with those obtained by QMC simulation of the Hubbard model in intermediate interaction regime [32], in a sense that QMC results in, a RVB liquid phase with no



broken symmetry for this region. Meng, *et. al.* have only calculated short range dimer-dimer correlation. Therefore this difference might be due to the fact that the geometry of finite clusters used in their simulation is not compatible with PL ordering. Based on present study, we believe that it is necessary to consider lattice geometries compatible with PL state and to calculate the plaquette-plaquette correlation for precise determination of the broken symmetries in the ground state.

## VII. ACKNOWLEDGMENT

Numerical analysis in this work have been carried out by Spinpack package [41]. This research was supported by the

Vice Chancellor for Research Affairs of the Isfahan University of Technology (IUT). S. A. J was supported by the National Elite Foundation (NEF) of Iran. We appreciate useful comments from G. Baskaran, A. Paramekanti, B. Kumar, M. Vojta, A. V. Chubakov.

- 
- [1] L. Balents, Nature **464**, 199 (2010).
  - [2] P. Fazekas and P. W. Anderson, Phil. Mag. **30**, 423 (1974)
  - [3] P. W. Anderson, Science, **235**, 1196 (1987)
  - [4] P. Fazekas, *Magnetism and electron correlations in strongly correlated systems*, World scientific (2001).
  - [5] F.D.M. Haldane, Phys. Rev. Lett., **50**, 1153 (1983)
  - [6] H. T. Diep and H. Giacomini in *Frustrated Spin Systems*, Ed. H. T. Diep, World Scientific (2004).
  - [7] A. Olariu. et al, Phys. Rev. Lett. **100**, 087202 (2008); H.Yoshida. et al, J. Phys. Soc. Jpn **78**, 043704 (2009); Y. Kurosaki. et al, Phys. rev. Lett. **95**, 177001 (2005); Y. Okamoto, H. Yoshida, and Z. Hiroi, J. Phys. Soc. Jpn. **78**, 033701 (2009); Z. Hiroi. et al, J. Phys. Soc. Jpn. **70**, 3377 (2001); T. Itou. et al, Phys. Rev. B **77**, 104413 (2008).
  - [8] D.A. Huse, Phys. Rev. B, **37**, 2380 (1988), D.A. Huse and V. Elser, Phys. Rev. Lett., **60**, 2531 (1988)
  - [9] J.D. Reger and A.P. Young, Phys. Rev. B, **37**, 5978 (1988)
  - [10] S. Tang and H.Q. Lin, Phys. Rev. B, **38**, 6863 (1988)
  - [11] J. Oitmaa and D.D. Betts, Can. J. Phys., **56**, 897 (1978)
  - [12] J.D. Reger, J.A. Riera and A.P. Young, J. Phys.: Condens. Matter, **1**, 1855 (1989)
  - [13] J. Oitmaa, C.J. Hamer and Z. Weihong, Phys. Rev. B, **45**, 9834 (1992)
  - [14] Z. Weihong, J. Oitmaa and C.J. Hamer, Phys. Rev. B, **44**, 11869 (1991)
  - [15] A. Auerbach, *Interacting Electrons and Quantum Magnetism*, Springer (1994).
  - [16] P. Chandra and B. Doucot, Phys. Rev. B, **38**, 9335 (1988); E. Dagotto and A. Moreo, Phys. Rev. Lett. **63**, 2148 (1989); D. Poilblanc, E. Gagliano, S. Bacci, and E. Dagotto, Phys. Rev. B **43**, 10970 (1991); H.J. Schulz and T. A. L. Ziman, Euro Phys. Lett., **18**, 355 (1992); P. Chandra, P. Coleman, and A. I. Larkin, Phys. Rev. Lett **64**, 88 (1990); M. P. Gelfand, R. R. P. Singh, and D. A. Huse, Phys. Rev. B **40**, 10801 (1989); O. P. Sushkov, J. Oitmaa, and Z. Weihong, Phys. Rev. B **66**, 054401 (2002); L. Capriotti, F. Becca, A. Parola, and S. Sorella, Phys. Rev. B **67**, 212402 (2003);
  - [17] F. Figueirido et al., Phys. Rev. B., **41**, 4619 (1989)
  - [18] N. Read and S. Sachdev, Phys. Rev. Lett., **66**, 1773 (1991)
  - [19] V. N. Kotov, et al, Phil. Mag. B., **80**, 1483 (2000)
  - [20] R.R.P. Singh et al, Phys. Rev. B., **60**, 7278 (1999)
  - [21] L. Capriotti and S. Sorella, Phys. Rev. Lett., **84**, 3173 (2000)
  - [22] A. Gellé, A. M. Läuchli, B. Kumar, and F. Mila, Phys. Rev. B, **77**, 014419 (2008)
  - [23] M. E. Zhitomirsky, Phys. Rev. B, **54**, 9007 (1996)
  - [24] M. Mambrini, A. Läuchli, D. Poilblanc, and F. Mila, Phys. Rev. B, **74**, 144422 (2006)
  - [25] J. B. Fouet, M. Mambrini, P. Sindzingere, and C. Lhuillier, Phys. Rev. B, **67**, 054411 (2003)
  - [26] I. Affleck, Phys. Rev. B., **37**, 5186 (1988)
  - [27] Y. Miura, R. Hiari, Y. Kobayashi, and M. Sato, J. Phys. Soc. Jpn., **75**, 084707 (2006)
  - [28] V. Kataev, A. Möller, U. Löw, W. Jung, N. Schittner, M. Kriener, and A. Freimuth, J. Magn. Magn. Mater., **290-291**, 310 (2005)
  - [29] O. Smirnova, et al, J. Am. Chem. Soc. **131** 8313 (2009); S. Okubo, et al, J. Phys. Conf. Ser. **200** 022042 (2010)
  - [30] S. Aubin, S. Myrskog, M. H. T. Extavour, L. J. LeBlanc, D. McKay, A. Stummer, and J. H. Thywissen, Nature Phys. **2**, 384 (2006).
  - [31] S. Inouye, M. R. Andrews, J. Stenger, H. J. Miesner, D. M. Stamper-Kurn, and W. Ketterle, Nature **392**, 151 (1998).
  - [32] Z. Y. Meng, T. C. Lang, S. Wessel, F. F. Assaad, A. Muramatsu, Nature **464** 847 (2010).
  - [33] T. Einarsson and H. Johannesson, Phys. Rev. B, **43**, 5867 (1991)
  - [34] J. B. Fouet, P. Sindzingere, C. Lhuillier, Eur. Phys. J. B., **20**, 241-254 (2001)
  - [35] N. Read, S. Sachdev, Phys. Rev. B., **42**, 4568 (1990)
  - [36] S. Katsura, T. Ide and T. Morita, J. Stat. Phys. **42**, 381 (1986)
  - [37] S. Okumura, H. Kawamura, T. Okubo and Y. Motome, J. Phys. Soc. Jpn. **79**, 114705 (2010).
  - [38] A. Mulder, R. Ganesh, L. Capriotti, and A. Paramekanti, Phys. Rev. B, **81**, 214419 (2010).
  - [39] S. M. Bhattacharjee, Z. Phys. B: Condensed Matter, **82** 323 (1991).
  - [40] Z. Noorbakhsh, F. Shahbazi, S. A. Jafari, G. Baskaran, J. Phys. Soc. Jpn. **78**, 054701 (2009).
  - [41] [www-e.uni-magdeburg.de/jschulen/spin/index.html](http://www-e.uni-magdeburg.de/jschulen/spin/index.html)